Applied Catalysis B: Environmental 142–143 (2013) 142–148

Contents lists available at SciVerse ScienceDirect

Applied Catalysis B: Environmental

journal homepage: www.elsevier.com/locate/apcatb

Photocatalytic reduction of Cr(VI) with TiO_2 film under visible light☆

Quanping Wu[b,c], Jun Zhao[b], Guohui Qin[a,*], Chengyang Wang[a], Xinli Tong[d], Song Xue[d,*]

[a] School of chemical Engineering, Tianjin University, Tianjin 300072, China
[b] School of Mechanical Engineering, Tianjin University, Tianjin 300072, China
[c] School of Electric Engineering, Tianjin University of Technology, Tianjin 300384, China
[d] School of Chemistry & Chemical Engineering, Tianjin University of Technology, Tianjin 300384, China

ARTICLE INFO

Article history:
Received 23 December 2012
Received in revised form 24 April 2013
Accepted 28 April 2013
Available online 14 May 2013

Keywords:
Photocatalytic reduction
Dye-sensitization
TiO_2 film
Chromium (VI)
Electron transfer

ABSTRACT

The performance of photocatalytic reduction of chromium (VI) via a new TiO_2 film and a platinum anode was systematically evaluated. The as-prepared TiO_2 film is composed of a dye-sensitized zone and a catalysis zone. Charge separation was accomplished with electron transferring to the catalysis zone and positive charge transforming to an anode. A powerful reduction ability of the reaction system was achieved in the absence of any organics under visible light irradiation. Several parameters including pH, dissolved O_2, the primary active species, the durability of the as-synthetized film and so on were investigated.

1. Introduction

Chromium is a toxic and mobile pollutant mainly originating from industrial processes like electroplating, leather tanning, and metallurgy [1,2]. It mainly occurs in two common oxidation states in aquatic environment, Cr(III) and Cr(VI). Cr(VI) species are known acutely toxic and carcinogenic, and one hundred times higher toxic than Cr(III) [3,4]. In addition, Cr(VI) is mobile in nature because of its weak absorption to inorganic surfaces [5]. In contrast, Cr(III) is readily precipitated at near-neutral pH, and it is much less mobile in the environment due to its highly "particle reactive"[6]. Removal of chromium from the environment has been actively investigated through many techniques such as cross flow microfiltration [7], reverse osmosis [8], ion exchange [9,10]. These methods were sometime expensive and often inefficient at low concentrations. Therefore, the preferred treatment of chromium pollutant in water is reduction of Cr(VI) to less harmful Cr(III), then readily occurs precipitation as $Cr(OH)_3$ in neutral or alkaline solutions [11].

Recently, photocatalytic reduction of Cr(VI) to Cr(III) using the semiconductor photocatalysis technology has received considerable attention [12–18]. Of all semiconductors, TiO_2 is the most frequently used photocatalyst due to its favorable chemical property, high stability, and relatively low cost [19]. Electron (e^-) and hole (h^+) are generated during the photolysis proceed of TiO_2. These photoelectrons and photoholes either recombine or become involved in redox reactions. The photo-excited electrons in DSC zone under light irradiation can arrive at catalysis zone rapidly [20], promoting the reduction of Cr(VI).During degradation of organics, the photoelectrons can attack O_2 to produce active species $O_2^{\bullet -}$, H_2O_2 and $^{\bullet}OH$ [21]. The photoholes with highly oxidizing ability can directly participate in oxidative degradation of organics or oxidizing water to produce $^{\bullet}OH$. These generated active species $O_2^{\bullet -}$, H_2O_2 and $^{\bullet}OH$ can degrade organics fully to CO_2 and water. Therefore, both photoelectrons and holes can play a role in the degradation of organic pollutants. For photocatalytic reduction of Cr(VI), electrons at the conduction band (CB) of TiO_2 reduce Cr(VI) to Cr(III). But the photoholes can not be used to reduce Cr(VI), and even produce $^{\bullet}OH$ from oxidation of water, which will oxidize Cr(III) to Cr(VI). In addition, the photoholes can not be used to reduce Cr(VI) similarly, and produce $^{\bullet}OH$ from oxidation of water, which will oxidize Cr(III) to Cr(VI). Meanwhile the serious electron-hole recombination causes its very slow reduction. Thus, organic compounds [22–26], such as methanol, ethanol, and acid, are often added as scavenger to suppress charge recombination and avoid the formation of $^{\bullet}OH$, thus leading to enhancement of the photoreduction. Alternatively, the photocatalytic reduction of Cr(VI) can be conducted in couple with the oxidation of organics by adding some organic pollutants in solution. Inorganic heavy metal ions and organic pollutants generally exist concurrently in actual pollution systems. Recently, the suspended TiO_2 powder has been proved to be an efficient photocatalyst for treatment of Cr(VI) waste

* Corresponding authors. Tel.: +86 22 60214250; fax: +86 22 60214252.
E-mail addresses: guohuiq163@sina.com (G. Qin), xuesong@ustc.edu.cn (S. Xue).

0926-3373/$ – see front matter © 2013 Elsevier B.V. All rights reserved.
http://dx.doi.org/10.1016/j.apcatb.2013.04.056

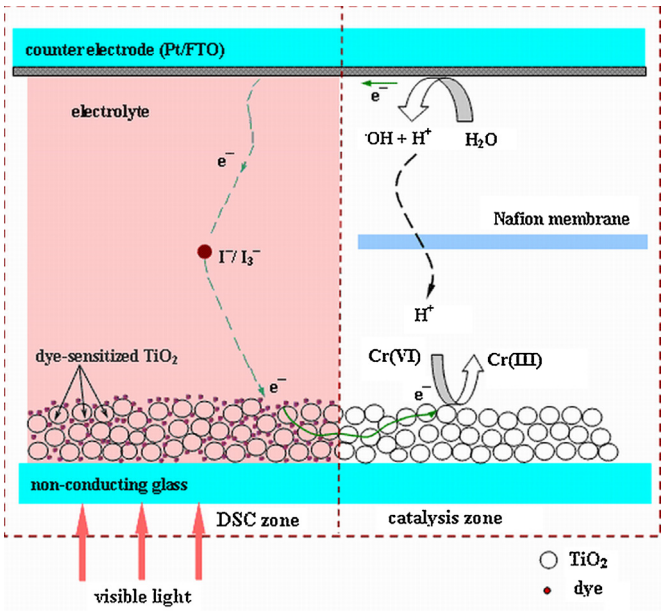

Fig. 1. Working mechanism for the photocatalytic reduction of Cr(VI).

water with organics. However, its UV light response of band gap 3.2 eV, penetration depth of UV light, filtration and re-suspension of these powders limit its practical application [27]. Moreover, it is evident that TiO_2 is not suitable for the treatment of single Cr(VI) waste water, which contains no or trace amount of organics at all. Hence, developing efficient and durable systems under visible light response for reduction of Cr(VI) becomes necessary.

Herein, we used a new TiO_2 film for photocatalytic reduction of Cr(VI) in aqueous solution under visible light irradiation. The as-prepared TiO_2 film was a composite of two zones, dye-sensitized (DS) zone and catalysis zone. In DS zone, a similar structure of dye-sensitized solar cells (DSCs) was fabricated, which was composed of a dye-sensitized TiO_2 film, electrolyte, and a counter electrode [28]. Light absorption and charge separation are finished in the DS zone. Electrons injected from dyes into CB of TiO_2 can diffuse from the DS zone to the catalysis zone along the network of TiO_2 nanoparticles. Any species with a reduction potential more positive than the CB of TiO_2 can consume these electrons in catalysis zone, among which the reduction of Cr(VI) to Cr(III) is inclined to be realized (Fig. 1). Besides, the high work efficiency through the TiO_2 film inspired us to verify the possibility of photocatalytic reduction of Cr(VI) in the absence of any organics [29–31].

2. Experimental

2.1. Apparatus

The new TiO_2 film was prepared according to the previous work [29]. The photocatalytic reduction of Cr(VI) experiment was implemented in a H-type reactor (Fig. 2). The catalysis zone with an activated area of 1.96 cm^2 was inserted into solution A containing $K_2Cr_2O_7$ aqueous solution (20 mg L^{-1}, 50 mL, pH 2). An electrode (Pt/FTO) with the same area acted as anode was inserted into solution B with 50 mL of distilled water. The two solutions were separated by Nafion membrane. The counter electrode of the TiO_2 was connected with the anode through a copper wire. A 300 W Xe lamp (λ_{max} = 500 nm) was used as the visible light source, which irradiated at a distance of 20 cm to the TiO_2 film surface through 420 nm cutoff filters. Light intensity, as measured by a visible-irradiance meter, was about 40 mW cm^{-2} at the position of the dye-sensitized region located. Air was bubbled through the pipe

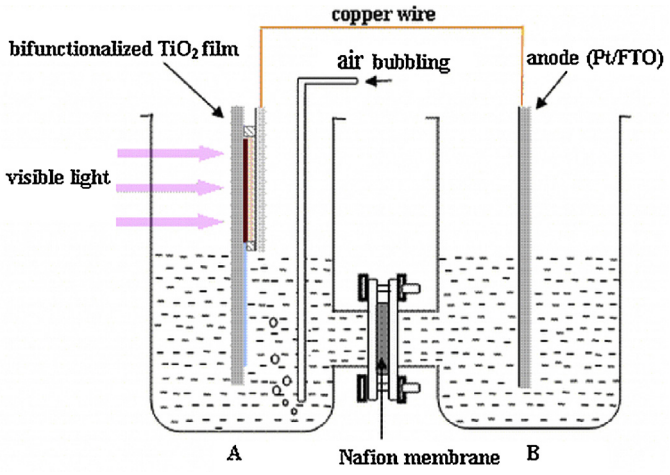

Fig. 2. Photocatalytic reduction of Cr(VI) in H-type reactor.

at a rate of 25 L h^{-1}, and gas flow was continued during irradiation. The initial pH in solution was adjusted by 2 M NaOH or 2 M H_2SO_4.

2.2. Chemical analysis

During the given time intervals, 1.0 mL of the sample was taken from the solution, and was analyzed for Cr(VI) using a 1.5-diphenylcarbazide (BDH) colorimetric method [32], determined spectrophotometrically by measuring the absorbance at 540 nm in acid solution with a UV–vis spectrophotometer (Varian). The concentration of phenol was determined by a HPLC using an Agilent 1100 chromatograph equipped with a ZORBAX Eclipse XDB-C18 reversed phase column. HPLC was detected by a UV detector adjusted to 270 nm. The mobile phase was a mixture of water and methanol (20:80 v/v) with a flow rate of 1.0 mL/min. The amounts of H_2 and O_2 was determined by GC/TCD. The concentration of Methyl orange(MO) in aqueous solution was monitored by UV/vis spectrophotometric measurements at given time intervals. Hydrogen peroxide concentration was determined by a spectrophotometric method using the potassium titanium (IV) oxalate method [33], and then the absorbance was measured at 400 nm in a 1 cm quartz cell. The fluorescence emission

Of 7-hydroxycoumarin was measured at 332 nm excitation using a spectro fluorometer.

3. Results and discussion

3.1. Effect of pH on the photoreduction of Cr(VI)

The pH of the solution is an important parameter in photocatalytic process. The reduction of chromium at different initial pH was shown in Fig. 3. The variation of pH had an obvious influence on the reduction of chromium (VI). Higher degradation efficiency was obtained when experiments were occurred in acidic solutions than that in alkaline solutions. The photoreduction efficiency dropped markedly with the increase of pH. For example, 99.5% of reduction efficiency was achieved at pH 2 after 60 min of visible light illumination, whereas 77% of Cr(VI) was reduced at pH 10 within the same time period. The effect of the acidified pH is in agreement with the reported results [34,35]. The dominant chromium species in the solution of pH 2 is $H_{CrO_4}^-$. The overall reduction reaction of $H_{CrO_4}^-$ can therefore be written as follows:

$$H_{CrO_4}^- + 7H^+ + 3e \underset{k_2}{\overset{k_1}{\rightleftharpoons}} Cr^{3+} + 4H_2O \quad (1)$$

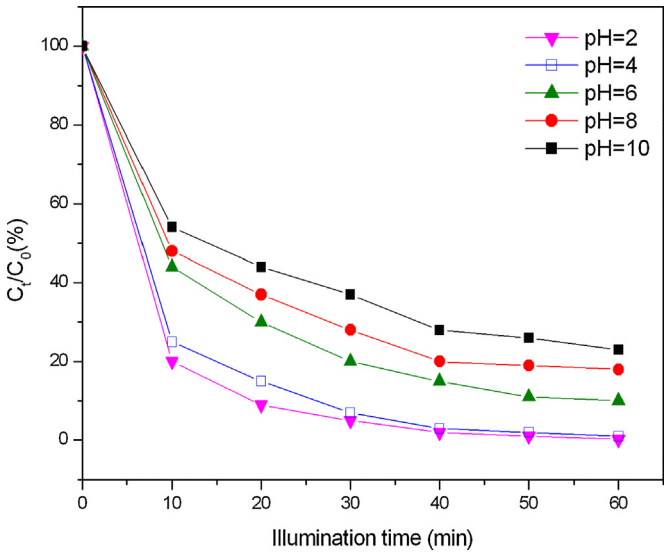

Fig. 3. Effect of pH on the reduction of Cr(VI) in solution (20 mg L^{-1}, 50 mL) with air bubbling.

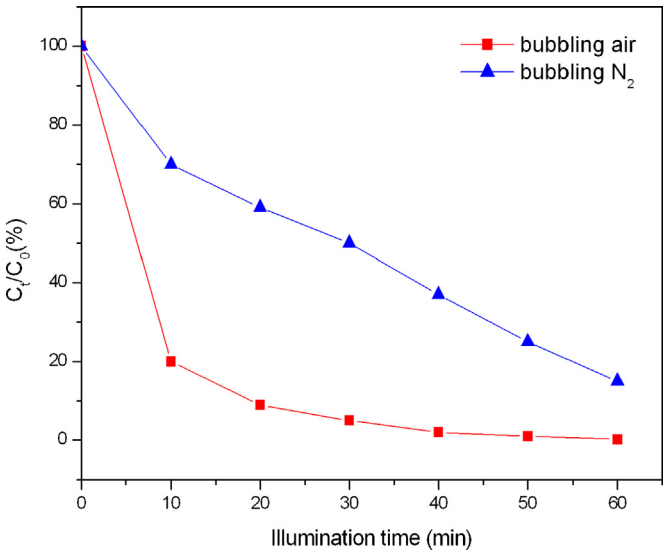

Fig. 4. Photoreduction of Cr(VI) in solution (20 mg L^{-1}, 50 mL, pH 2) when bubbling air or N_2.

$$K = k_1 k_2^{-1} \quad (2)$$

$$k_1 = C_{HCrO_4^-} C_{H^+} C_{Cr^{3+}}^{-1} \quad (3)$$

$$k_2 = C_{Cr^{3+}} C_{H^+}^{-1} C_{HCrO_4^-}^{-1} \quad (4)$$

K, k_1, k_2 express the overall reaction rate constant, positive reaction rate constant and negative reaction rate constant, respectively, while $C_{HCrO_4^-}$, $C_{Cr^{3+}}$, C_{H^+} refer to the Cr(VI) concentration, the Cr(III)concentration and the H^+ concentration, respectively. Since the overall reaction rate constant is fixed at room temperature, the higher concentration of protons (H^+) at lower pH value will cause higher positive reaction rate constant and will benefit the reaction Eq. (1) shifting to the right side. Hence, the thermodynamic driving force of electrons from CB to Cr(VI) increases with pH's decreasing. In addition, the reduction potential of the couple Cr^{6+}/Cr^{3+} moves more positive at low pH than the CB of TiO_2 shifts [36]. Besides, TiO_2 surface becomes positively charged under acidic $HCrO_4^-$ shows high adsorption capacity at low pH [37]. These reasons might result in high reduction efficiency of Cr(VI) in acidic condition. Of course, the deposition of $Cr(OH)_3$ on the catalyst surface under neutral or alkaline conditions retards the photoreduction, which can not be ignored.

3.2. *Effect of bubbling air and N_2 gas*

To study the effect of O_2 in the photoreduction of Cr(VI) on the TiO_2 film, experiments were carried out under bubbling air or nitrogen gas. As shown in Fig. 4, the photocatalytic efficiency was higher in air (99%) than in N_2 (85%) case. The presence of oxygen contributes significantly to the photocatalytic process. O_2 may act as both an electron scavenger and a source of reductant. As an electron scavenger, O_2 competes with Cr(VI) for the photogenerated electrons at CB of TiO_2, which will decrease the Cr(VI) reduction rate. As for a source of reductant, it is well known that O_2 can react with electrons at CB of TiO_2 to produce $O_2^{\bullet -}$, followed by reaction with H^+ to form $^\bullet$OOH, $^\bullet$OH and H_2O_2(Eqs. (5)–(8)). The species $O_2^{\bullet -}$, $^\bullet$OOH and H_2O_2 possess oxidizing ability, they can also act as reductant when reacting with Cr(VI) [38,39]. Consequently, in the presence of O_2, Cr(VI) can be directly reduced by the photoelectrons or indirectly by the photogenerated $O_2^{\bullet -}$, $^\bullet$OOH and H_2O_2. It should be noted that highly active species of hydroxyl radicals $^\bullet$OH formed from O_2 will oxidize Cr(III) to Cr(VI). Some controversial results are obtained by different authors [11,40]. The higher reduction efficiency of Cr(VI)(Fig. 4) observed suggests that the formation of $O_2^{\bullet -}$, $^\bullet$OOH, H_2O_2 (Eq. (5), Eq. (6), Eq. (7)) possibly was predominate during the reduction reaction, whereas the formation of HO$^\bullet$ (Eq. (8)) was subordinate.In contrast, the formation of HO$^\bullet$ was chiefly during the oxidation reaction.

$$O_2 + e_{CB}^- \rightarrow O_2^{\bullet -} \quad (5)$$

$$O_2^{\bullet -} + H^+ + e_{CB}^- \rightarrow HOO^\bullet \quad (6)$$

$$HOO^\bullet + H^+ + e_{CB}^- \rightarrow H_2O_2 \quad (7)$$

$$H_2O_2 + e_{CB}^- \rightarrow HO^- + HO^\bullet \quad (8)$$

The photodegradation of Methyl orange (MO) and the Cr(VI) reduction were conducted in H-type reactor under the same condition (20 mg L^{-1},pH 2) concurrently for the purpose of testing the assume. The formation of hydrogen peroxide (H_2O_2) was detected. Coumarin was added as a reagent trap of $^\bullet$OH to form the production of the coumarin-OH adduct (7-hydroxycoumarin), which can be quantified by measuring its fluorescence emission intensity [41]. The results in the two groups were shown in Fig.S1, Fig.S2, Fig.S3 and Fig.S4.As depicted in Fig.S1,the amounts of H_2O_2 produced during the progress of Cr(VI) reduction was much higher than that in oxidation of MO, whereas the concentration of $^\bullet$OH was much weaker comparing with the oxidation reaction (Fig.S2, Fig.S3)accordingly.Fig.S4 depicted that the degradation of MO was performed fully. The two possible degradation pathways for methyl orange was proposed in scheme 1 (for more details, see supporting information). The hydroxyl radical attack was involved in both pathways. From these results it was convinced that the major active species was $O_2^{\bullet -}$, $^\bullet$OOH and H_2O_2 during the Cr (VI) reduction progress while the predominate active species was $^\bullet$OH during the MO degradation progress. Therefore, Cr(VI) trended to be reduced into Cr(III) rather than Cr(III) occured oxidation into Cr(VI),which is in accordance with the thermodynamic driving force result at lower pH.

Under N_2-atmosphere, a greater amount of Cr(VI) might be photoreduced compared to that under air-equilibration. However, a decrease has been found in photoreduced Cr(VI) when bubbling

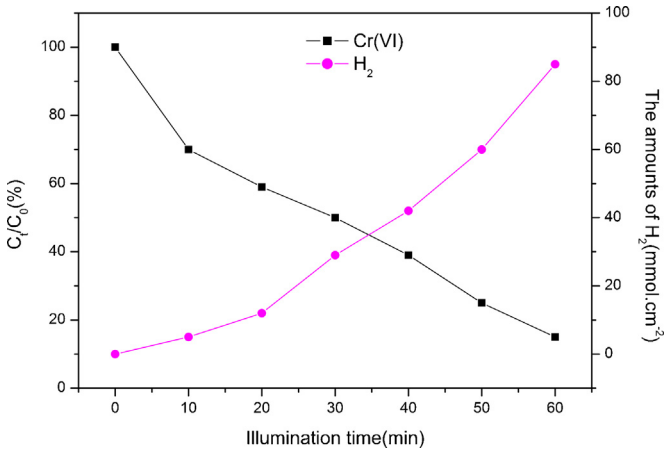

Fig. 5. Effect of Cr(VI) reduction and the amounts of hydrogen production accomplishment concurrently.

N_2. There may be existing another competing reaction between reduction of Cr(VI) and H_2 evolution.

With the purpose of further verifying the postulation, the investigation of H_2 was carried out subsequently. A closed gas-circulation system was connected to H-type reactor of solution A, and H_2 was measured using an online GC/TCD. The H_2 evolution and the variation of Cr(VI) concentration as function of irradiation time at N_2 atmosphere was shown concurrently in Fig. 5. As depicted in Fig. 5, considerable H_2 was observed, weighed by activated area, accounting to 85 mmol cm^{-2} at 1 h. The variation of Cr(VI) decreases obviously while the amounts of the photocatalytically produced H_2 increases sharply with the exposure time, which is in accordance with the araised assume. The protons absorbed on TiO_2 surface can accept CB electrons to produce hydrogen. As the concentration of $HCrO_4^-$ declines, the reduction of H^+ ion will become predominant and more electrons take part in hydrogen production. Thus, the competition with H_2 evolution leads to decrease of the photoreduction of Cr(VI). These results suggest that O_2 is beneficial to the photoreduction of Cr(VI) because O_2 acts as the carrier of electron transfer and suppresses H_2 evolution to some extent, particularly at low concentration of Cr(VI).

3.3. Effect of initial concentration of Cr(VI)

The rate of photo-reduction of Cr(VI) over the TiO_2 film was studied by setting the initial concentration of Cr(VI) in the range of 10–50 mg L^{-1}. As depicted in Fig. 6, Cr(VI) reduction efficiency gradually decreases with the increase of the initial concentration of Cr(VI) from 10 to 50 mg L^{-1}. After 60 min, the percentage of Cr(VI) drops 99% at concentration of 10 mg L^{-1} and 86% at concentration of 50 mg L^{-1} under the same conditions of photoreduction. Then, the kinetics of the photocatalytic reduction of Cr(VI) were investigated. As seen in Fig. 7, a linear relationship was observed between Cr(VI) concentration and irradiation time. The kinetic data calculated from the obtained results can be fitted to a rate expression of a pseudo-first-order reaction [11,38]: $\ln(C_0/C_t) = -k_{Cr}t$, where C_0 represents the initial Cr(VI) concentration and C_t refers to the Cr(VI) concentration at irradiation time (t), and k_{Cr} is the apparent rate constant of the photocatalytic reduction of Cr(VI). The rate constant values were found to decrease with the increase of initial Cr(VI) concentration from 20 to 50 mg L^{-1}. Since the light intensity and TiO_2 film were fixed, the same active sites in DS zone and catalysis zone cause a decrease in the initial rate of photoreduction of Cr(VI) with concentration's increasing.

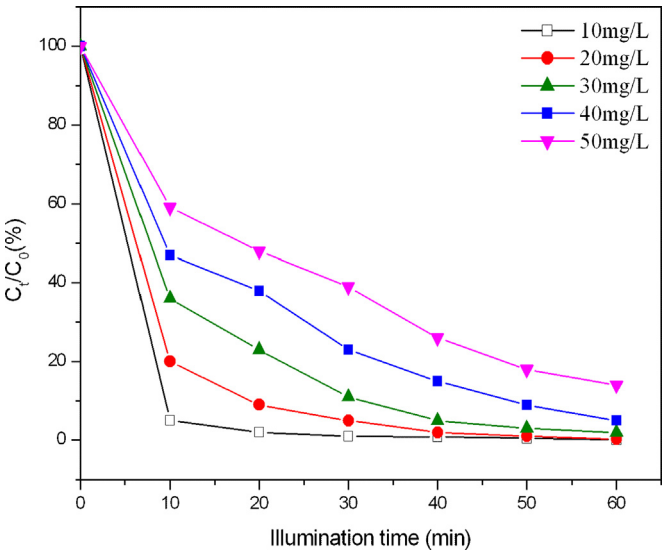

Fig. 6. Effect of initial concentration of Cr(VI) on the photoreduction in solution (20 mg L^{-1}, 50 mL, pH 2) with air bubbling.

3.4. Durability of the new TiO_2 film

Considering the practical application, the durability of the TiO_2 film was tested when the reaction was carried out in solution (20 mg L^{-1}, 50 mL, pH 2) under visible light illumination. The removal efficiency of chromium(VI) was decreased 3%, from 99% to 96%, during running 6 cycles. The results demonstrated the as-prepared TiO_2 film was comparably stable under the studied conditions. Further study was conducted in 800 mL solution (20 mg L^{-1}, pH 2) to evaluate the photocatalytic capability of the TiO_2, and the results were revealed in Fig. 8. The concentration of Cr(VI) decreased gradually with illumination time's rising. After 6 h, the photocatalytic efficiency was obtained with 98% removal of Cr(VI) in the examined 800 mL solution. Due to its good stability and large capacity, it is feasible for the TiO_2 film to be applied in large scale photocatalytic reduction of Cr(VI) using solar light. Furthermore, the photoreduction of Cr(VI) based on the TiO_2 was carried out without any organics as scavenger.

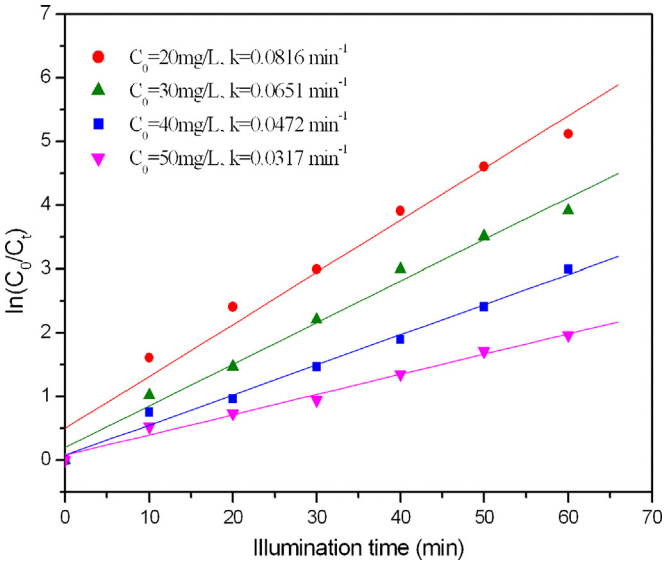

Fig. 7. Plot of $\ln(C_t/C_0)$ versus time for photo-reduction of Cr(VI).

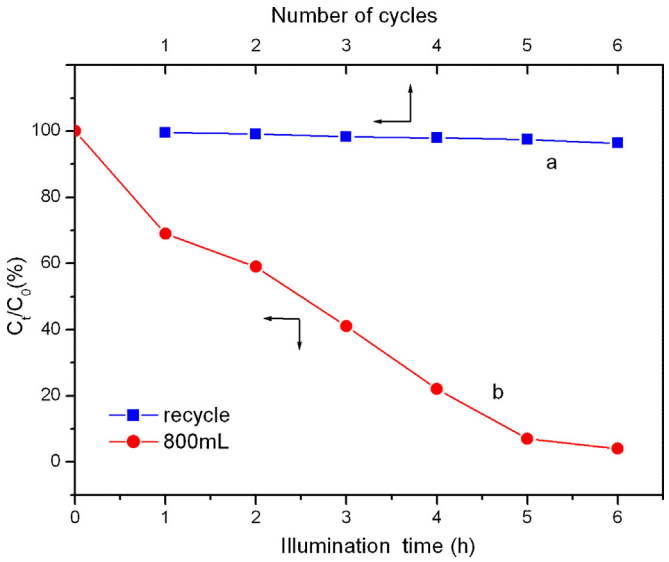

Fig. 8. The removal efficiency of Cr(VI) at running 6 cycles in solution (20 mg L^{-1}, 50 mL, pH 2) (a); photoreduction conducted in 800 mL solution (20 mg L^{-1}, pH 2) (b).

3.5. Effect of organics on the photoreduction

The Cr(VI) waste water often contains organic pollutants in actual pollution systems. It has been reported that the presence of organic compounds as sacrificial electron donor can accelerate the photocatalytic reduction of Cr(VI) [22–26]. The photogenerated holes are rapidly scavenged from the TiO_2 particles by the organic species, suppressing electron–hole recombination on TiO_2 and accelerating the reduction by photogenerated electron. From the view point of the photocatalytic treatment of both organic and inorganic waste water, the effect of phenol added to the reduction system was investigated in this work. The addition of phenol is expected to act as electron donor to promote the photoreduction. One experiment is designed under the condition of adding phenol to solution B, in which anode was inserted. The reaction was carried out in H-type reactor with solution A (Cr = 20 mg L^{-1}, V = 50 mL, pH = 2) and solution B (phenol = 20 mg L^{-1}, V = 50 mL, pH = 2) under visible light. As reflected in Fig. 9, the photocatalytic efficiency was

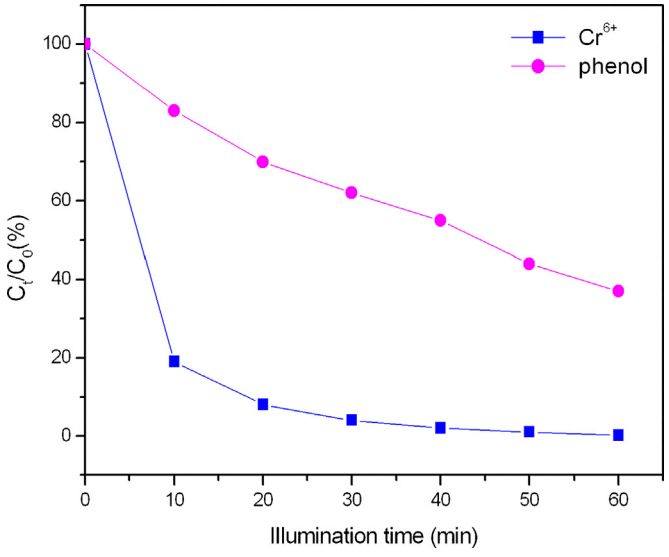

Fig. 9. Photocatalytic efficiency of Cr^{6+} in solution A and degradation of phenol in solution B when phenol was added in solution B.

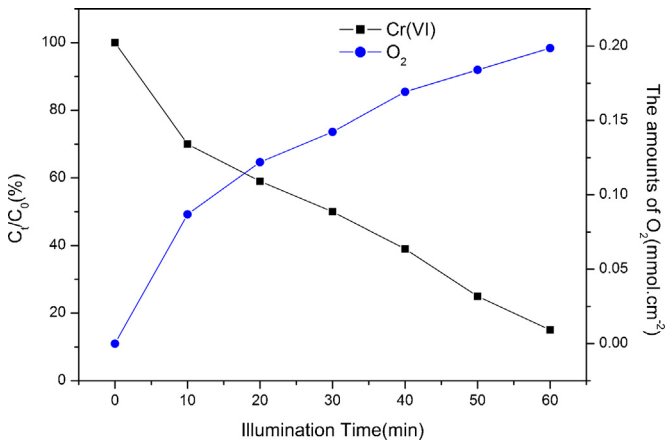

Fig. 10. The amounts of O_2 production and the variation of Cr(VI) concentration.

as high as 99% after 60 min illumination. The photoreductions of Cr(VI) are similar in the presence and the absence of phenol in solution B. The results revealed that phenol added in solution B had no obvious influence on the reduction of Cr(VI). It was also found that the concentration of phenol decreased with time and 63% removal of phenol was obtained after 60 min. Previous report exhibits that anode directly oxidizes phenols via its oxidation ability or oxidizes water to produce hydroxyl radical •OH, which is highly active for degradation of organics [30]. The oxidation ability of the anode is derived from the dye-sensitized zone of TiO_2 film. Under light excitation and after electron injected to CB of TiO_2, dye is oxidized to dye^+. The dye^+ is regenerated by stripping electron from I^- in electrolyte, oxidizing it into I_3^-, which results in separation of electron and positive charge. Therefore, charge recombination is suppressed by the efficient charge separation through the controlled DSCs structure design, rather than by electron donor of organics. When I_3^- is catalytically converted into I^- through counter electrode with electron exchange, the positive charge is transported from counter electrode to anode through copper wire.

As dyes repeated the process cycle of light absorption and regeneration, the oxidation potential of anode becomes high enough for water oxidation, producing •OH, proton, and electron (Eq. (9)), or leading to generation of O_2 in the absence of any organics (Eq. (10)).

$$Pt + H_2O \rightarrow Pt(^{\bullet}OH) + H^+ + e^- \quad (9)$$

$$Pt + H_2O \rightarrow Pt(O_2) + 2H^+ + 2e^- \quad (10)$$

In our previous paper [30], the coumarin-OH adducts were measured in proportion to the illumination time, proving that hydroxide radicals were indeed generated. The concrete amount of oxygen evolved by anode was also tested by the same investigation method of H_2 (Fig. 10). The evolution of O_2 increases gradually with the decreasing of Cr(VI), reaching 198 mmol cm^{-2} after 1 h exposure. Other experiments are carried out under conditions of phenol added to solution A with air or nitrogen gas case, and the experimental results are put forward in Fig. 11. When bubbling air, the photocatalytic reduction of Cr(VI) worked smoothly at starting stage, but it became slowly after 40 min compared to the absence of phenol, and causing a bit lower reduction efficiency within 60 min (87% versus 99%). The phenol added in solution A diminished the photocatalytic reduction of Cr(VI), which may be ascribed to the presence of O_2. The $O_2^{\bullet-}$, •OOH and H_2O_2 generated from the reaction of oxygen and electron can act as reductant to reduce Cr(VI) from the initial concentration. When Cr(VI) is reduced with illumination time and presents at low concentration, the species $O_2^{\bullet-}$, •OOH and H_2O_2 might be mainly focused on dealing with phenol

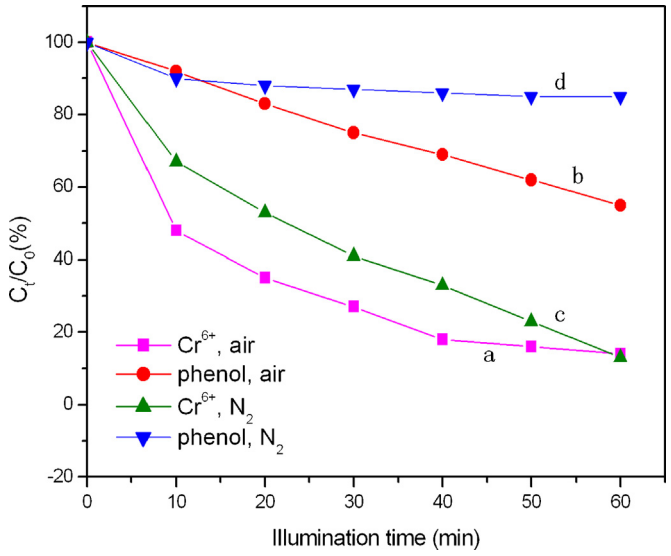

Fig. 11. Photocatalytic efficiency of Cr^{6+} (20 mg L^{-1}) and phenol (20 mg L^{-1}) in solution A (pH 2) with bubbling air (a, b) and N_2 (c, d).

through their oxidizing ability. The 45% removal of phenol further proves the oxidation reaction involved by these species, which will exhaust some amounts of reductant for reduction of Cr(VI), and decrease the Cr(VI) reduction efficiency. When Cr(VI) was at a low concentration of 4 mg L^{-1}, the addition of phenol (20 mg L^{-1}) in solution A markedly lowered the reduction of Cr(VI) with only 21% Cr(VI) removal after 60 min. These results suggested that the photoreduction of Cr(VI) was suppressed by the presence of phenol, particularly seriously at low concentration of Cr(VI) when Cr(VI) and phenol were coexistent in a solution.

Under nitrogen atmosphere, the similar photocatalytic reductions of Cr(VI) were obtained both in the presence and the absence of phenol (line c in Fig. 11 vs Fig. 4), which shows that the addition of phenol has no effect on the reduction of Cr(VI) under nitrogen. On the other hand, only 15% of phenol was removed after 60 min (line d in Fig. 11). The small removal of phenol may be partly owning to the absorption of TiO_2 surface or the effect of minimal adsorbed oxygen on the surface of TiO_2. These results demonstrate that active species, such as $O_2^{\bullet-}$ and $^{\bullet}OH$, were hardly formed at nitrogen ambient, thus leading to little degradation of phenol and electrons at CB of TiO_2 as reductant reduced Cr(VI) to Cr(III) directly.

3.6. *The test of electrons in catalysis zone*

The new TiO_2 film containing DSC zone and catalysis zone works smoothly during the reduction of Cr(VI). In DSC zone, light absorption and charge separation are accomplished according to the principle of DSC. In catalysis zone, the electron on conduction band of TiO_2 transforms from DSC zone to catalysis zone and converts Cr(VI) into Cr(III) under the catalysis of nano TiO_2. The separated positive charges transfer through electrolyte to anode and oxidize water to release O_2 to atmosphere. To provide evidence about electron passing along TiO_2 film into catalysis zone, the current in catalysis zone was measured by electrochemical workstation. The absorption spectra of N719 dye adsorbed on TiO_2 films was firstly tested in order to investigate the optimum LED (Fig. S5). As shown from Fig. S5, the dye displays two absorption bands at around 360 nm and 526 nm, which mainly stem from the intramolecular charge-transfer transition when light illumination on DSC zone is turning on. The intensity of visible light should be related to local electron density, and high electron density will lead to strong absorbance and subsequently high electron intensity. The

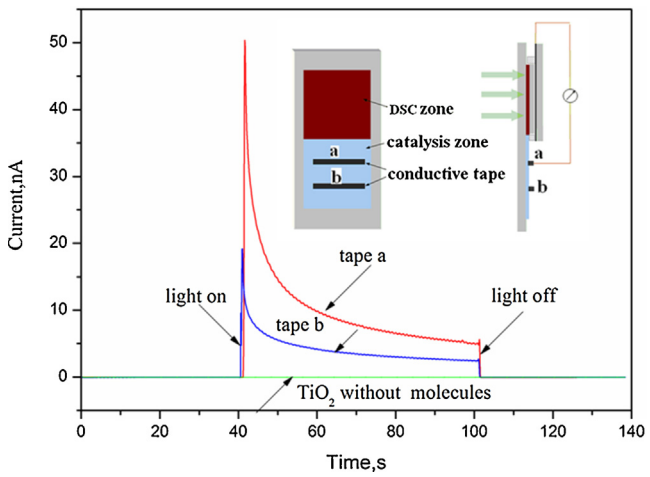

Fig. 12. The absorption spectra of N719 dye adsorbed on TiO_2 films.

DSC zone and catalysis zone of the TiO_2 film were illuminated with a 525 nm LED, and their following currents results for tapes *a* and *b* measured occur after light on, and sharply decrease to initial state after light off, whereas the current for TiO_2 film without dye molecules remains nearly unchanged when under light illumination (Fig. 12), in which dye molecules have an important effect on the behavior of absorbing visible light. These results provided clear evidence that electrons indeed pass along the as–synthetized films from DSC zone into catalysis zone.

4. Conclusions

The ability of the new TiO_2 film for the Cr(VI) reduction under visible light has been demonstrated. The removal efficiency of Cr(VI) was higher in acidic solutions than that in alkaline solutions. High removal efficiency was achieved in the absence of any organics within 1 h at pH 2. Oxygen acted as the source of reductant for enhancement of the photo-reduction. Phenol added into anode solution as electron donor was expected to promote photocatalytic reduction. But it turned out to have no effect on the reduction of Cr(VI). When phenol was added into the Cr(VI) solution, the oxidation reaction of phenol completed with the reduction of Cr(VI), thereby decreased the photoreduction, and this was especially serious at low concentration of Cr(VI). The good durability and the large capacity will benefit the TiO_2 film for removal of chromium (VI) under environmentally favorable conditions.

Acknowledgments

We are grateful to the National Natural Science Foundation of China (21072152, 21101115) for financial supports.

Appendix A. Supplementary data

Supplementary data associated with this article can be found, in the online version, at http://dx.doi.org/10.1016/j.apcatb.2013.04.056.

References

[1] Y. Gong, X. Liu, Journal Hazardous Materials 179 (2010) 540–544.
[2] M. Gheju, A. Iovi, I. Balcu, Journal Hazardous Materials 153 (2008) 655–662.
[3] M. Costa, Toxicology and Applied Pharmacology 188 (2003) 1–5.
[4] V. Kapil, Chromium toxicity, in: U.S. Department of Health and Human Services, Public Health Services, vol. 2–3, Agency for Toxic Substances and Disease Registry, Atlanta, GA, 1990, pp. 16–17.
[5] M.E. Losi, C. Amrhein, W.T. Frankenberger Jr., Reviews of Environmental Contamination and Toxicology 136 (1994) 91.

[6] L. Calder, Chromium in the natural and human environments, in: J.O. Nriagu, E. Nieboer (Eds.), Advances in Environmental Science and Technology, vol. 20, Wiley & Sons, New York, 1988, pp. 215–230.
[7] U. Danis, Desalination 181 (2005) 135–143.
[8] C. Das, P. Patel, S. De, S.D. Gupta, Separation and Purification Technology 50 (2006) 291–299.
[9] A.A. Atia, Journal of Hazardous Materials 137 (2006) 1049–1055.
[10] G. Tiravanti, D. Petruzzelli, R. Passiono, Water Science & Technology 36 (1997) 197–207.
[11] D.P. Das, K. Parida, B.R. De, Journal of Molecular Catalysis A: Chemical 245 (2006) 217–224.
[12] J.J. Testa, M.A. Grela, M.I. Litter, Environment Science & Technology 38 (2004) 1589–1594.
[13] A. Kleiman, A. Marquez, M.L. Vera, J.M. Meichtry, M.I. Litter, Applied Catalysis B: Environmental 101 (2011) 676–681.
[14] R. Vinu, G. Madras, Environment Science & Technology 42 (2008) 913–919.
[15] R. Mu, Z. Xu, L. Li, Y. Shao, H. Wan, S. Zheng, Journal of Hazardous Materials 176 (2010) 495–502.
[16] H. Yu, S. Chen, X. Quan, H. Zhao, Y. Zhang, Environment Science & Technology 42 (2008) 3791–3796.
[17] S. Luo, Y. Xiao, L. Yang, C. Liu, F. Su, Y. Li, Separation and Purification Technology 79 (2011) 85–91.
[18] L. Yang, Y. Xiao, S. Liu, Y. Li, Q. Cai, S. Luo, Applied Catalysis B: Environmental 94 (2010) 142–149.
[19] A. Fujishima, T.N. Rao, A. Tryk, Journal of Photochemistry and Photobiology C: Photochemistry Reviews 1 (2000) 1–21.
[20] F.A. Folusho, K.-Y. Kim, K.-J. Chae, M.-J. Choi, S.-Y. Kim, I.-S. Chang, I.-S. Kim, International Journal of Hydrogen Energy 34 (2009) 9297–9304.
[21] U.I. Gaya, A.H. Abdullah, Journal of Photochemistry and Photobiology C: Photochemistry Reviews 9 (2008) 1–12.
[22] G. Kim, W. Choi, Applied Catalysis B: Environmental 100 (2010) 77–83.
[23] N. Wang, L. Zhu, K. Deng, Y. She, Y. Yu, H. Tang, Applied Catalysis B: Environmental 95 (2010) 400–407.
[24] N. Wang, Y. Xu, L. Zhu, X. Shen, H. Tang, Journal of Photochemistry and Photobiology A: Chemistry 201 (2009) 121–127.
[25] J. Sun, J.-D. Mao, H. Gong, Y. Lan, Journal of Hazardous Materials 168 (2009) 1569–1574.
[26] L. Wang, N. Wang, L. Zhu, H. Yu, H. Tang, Journal of Hazardous Materials 152 (2008) 93–99.
[27] D. Chen, F. Li, A.K. Ray, AIChE Journal 46 (2000) 1034–1045.
[28] A. Hagfeldt, M. Grätzel, Accounts Chemical Research 33 (2000) 269–277.
[29] G.H. Qin, Z. Sun, Q.P. Wu, L. Lin, M. Liang, S. Xue, Journal of Hazardous Materials 192 (2011) 599–604.
[30] G.H. Qin, Q.P. Wu, Z. Sun, W. Ying, J.Z. Luo, S. Xue, Journal of Hazardous Materials 199 (2012) 226–232.
[31] G.H. Qin, Y. Zhang, X.B. Ke, X.L. Tong, Z. Sun, M.L. iang, S. Xue, Photocatalytic reduction of carbon dioxide to formic acid, formaldehyde, and methanol using dye-sensitized TiO_2 film, Applied Catalysis B: Environmental 129 (2013) 599–605.
[32] X. Zhou, T. Korenaga, T. Takahashi, T. Moriwake, S. Shinoda, Water Research 27 (1993) 1049–1054.
[33] R.M. Sellers, Analyst 150 (1980) 950–954.
[34] J. Munoz, X. Domenech, Journal of Applied Electrochemistry 20 (1990) 518–521.
[35] W. Lin, C. Wei, K. Rajeshwar, Journal of the Electrochemical Society 140 (1993) 2477–2482.
[36] X.L. Wang, S.O. Pehkonen, A.K. Ray, Industrial & Engineering Chemical Research 43 (2004) 1665–1672.
[37] J.M.A. Gimknez, S. Aguado, Journal of Molecular Catalysis A: Chemical 105 (1996) 67–78.
[38] Y. Ku, I.L. Jung, Water Research 35 (2001) 135–142.
[39] L.B. Khalil, W.E. Mourad, M.W. Rophael, Applied Catalysis B: Environmental 17 (1998) 267–273.
[40] H.L. Liu, Y. Zhou, H.Y. Huang, Y.Y. Feng, Desalination 278 (2011) 434–437.
[41] J.W. Kim, C.L. Lee, W.Y. Choi, Environment Science & Technology 44 (2010) 6849–6854.